# Laser-induced-fluorescence imaging of NO in a eta-heptane- and diesel-fuel-driven diesel engine

Appl. Phys. B 57, 405–410 (1993)

Applied Physics B Photophysics and Laser Chemistry



# Laser-Induced-Fluorescence Imaging of NO in an $n$-Heptane- and Diesel-Fuel-Driven Diesel Engine

**Th. M. Brugman**[1], **R. Klein-Douwel**[1], **G. Huigen**[2], **E. van Walwijk**[2], **J. J. ter Meulen**[1]

[1] Department of Molecular and Laser Physics, University of Nijmegen, Toernooiveld, 6525 ED Nijmegen, The Netherlands
[2] Laboratory for Automotive Engineering, University of Eindhoven, P.O. Box 513, 5600 MB Eindhoven, The Netherlands

Received 1 June 1993/Accepted 6 August 1993

**Abstract.** Continuous on-line imaging by 2D-LIF techniques of in-cylinder NO distributions in a running Diesel engine is explored using an ArF-excimer laser at 193 nm operating at low power. For the first time NO excitation spectra could be measured as a result of high optical transparencies during measurements over longer periods of time. The averaged distributions show different combustion behaviour of both fuels proving the potential of the 2D-LIF technique in application to non-intrusive combustion diagnostics in a steady running Diesel engine.

**PACS:** 42.30, 82.20

The study of the combustion process inside the combustion chamber of a Diesel engine is of utmost importance for the reduction of toxic emission components like NO and soot particles. Although modelling of the combustion process continues to progress, we are still far from a profound understanding of the physics and chemistry inside the engine. At the moment the design of Diesel engines is still mainly based on empirically obtained knowledge. In view of the complexity of the Diesel fuel combustion process, any information about where and when NO or soot is produced, is extremely valuable. This information can, in principle, be obtained by using non-intrusive diagnostic laser techniques.

During the last decade the Laser-Induced Fluorescence (LIF) method has proven its powerful value as a sensitive and molecule selective detection technique in application to both stationary as well as turbulent combustion processes, as indicated by numerous publications on this topic. The LIF method has been applied successfully to spark ignition car engines [1] and recently also to the observation of molecular distributions inside a running Diesel engine. Arnold et al. [2] were the first to demonstrate that two-dimensional distributions of NO and OH can be recorded by LIF using a tunable excimer laser at 193 nm and 248 nm, respectively. Recently also Alatas et al. [3] have visualised the NO distribution by LIF applying a frequency-doubled tunable dye laser at 226 nm. They concluded that the NO formation starts early during combustion and stops no later than 30 to 40 degrees a.TDC (after Top Dead Centre).

In both investigations a Diesel engine was used running on a substitute fuel, $n$-heptane [2] or a 50/50 mixture of isooctane and tetradecane [3] (chosen for its combustion properties resembling those of real Diesel fuel). The main reason for not using Diesel fuel is the presence of numerous absorbing and fluorescing components causing a low transmission of the laser beam and a strong combustion background radiation in a large wavelength region. Another very serious problem in the case of Diesel fuel is the high soot production causing a blackening of the windows and reflection of the laser light by the soot particles. However, the soot problem is not eliminated by combusting substitute fuels. In the two experiments mentioned above, the windows could be kept clean during one or two minutes. This is too short to record excitation spectra to characterize the measured species. Furthermore, any study of the NO distributions as a function of varying combustion conditions (e.g. engine load, rotational speed and operating temperature) will be difficult since the engine has to be stopped and opened after each measurement in order to clean the windows. Restarting the engine almost certainly leads to slightly different combustion conditions during the measurements since there will be too little time to reach steady equilibrium conditions.

The objective of the present investigation is the study of the possibility of LIF diagnostics of NO inside a Diesel engine running on both $n$-heptane as well as Diesel fuel. In contrast to the experiments of Arnold et al. and Alatas et al., an indirectly injected Diesel engine is used. The optical access also differs from the transparent engine setup used by these authors. The results make clear that the LIF technique using a tunable excimer laser offers very promising perspectives for the observation of NO, even in the combustion of Diesel fuel. Excitation spectra are obtained which undoubtedly belong to NO. The measurements are performed at specific crank angles as a function of engine load. As may be expected, the NO distributions in $n$-heptane and Diesel fuel combustion show some clear differences. Essential for all these 2D-LIF measurements is the avoidance of window blackening, thereby extending the measurements to a nearly unlimited period of time.

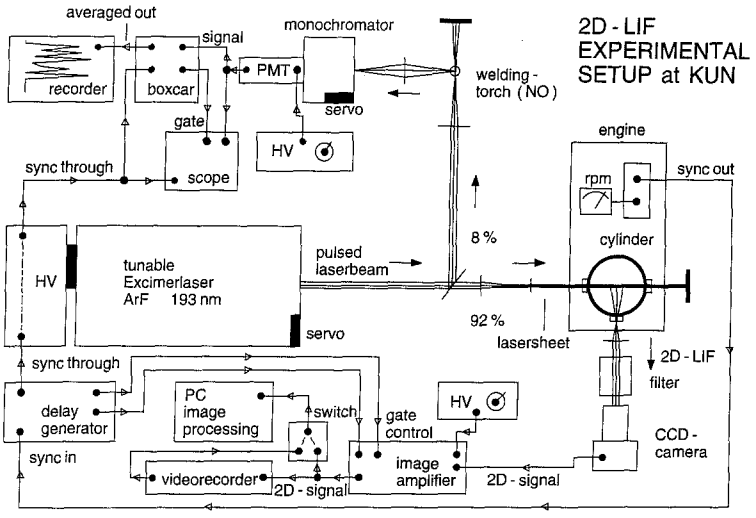


**Fig. 1.** Schematic overview of the experimental setup

## 1 Experimental

A schematic overview of the experimental setup is depicted in Fig. 1. The measurements are performed in a 4-stroke air-cooled single cylinder indirectly injected Diesel engine (HATZ-Samofa) with a swept volume of 581 cc (bore 86 mm, stroke 100 mm). The internal timing is performed by unadjustable cams on the cam-shaft, leaving the amount of fuel supplied each full cycle as the only controllable variable of the engine. An adjustable water-cooled electric brake (Zollner & Co.) is mounted on the engine by means of a flexible shaft attached directly to the flywheel, thus providing the various load conditions. The engine is lubricated by a minimized amount of a UV-transparent and chemically inert lubricant in order to prevent engine damage during the measurements. The synchronization of the laser pulses to the running engine is performed by an opto-electronic device which continuously monitors the rotation of the cam-shaft. This device triggers the delay generator (SRS DG 535) which synchronizes the laser and the detection system. The rotational resolution is about 0.6° and since in a 4-stroke engine the crank rotates at twice the speed of the cam-shaft, the error made in any selected crank angle is found to be 1.2°. The rotational speed of the crank is determined by an on-line display of the angular frequency. The influence of oxygen enriched combustion on the NO and soot formation, as reported by Alatas et al. [3] and others, is verified by means of an adjustable oxygen supply to the air-inlet of the engine.

The interior of the cylinder is made optically accessible by mounting three cylindrical quartz windows in the cylinder wall as close to the cylinder head as possible. A sketch of the modified cylinder is depicted in Fig. 2. Due to the discrepancy of the flat inner surface of each window (diameter 25 mm) and the curvature of the cylinder wall, a part of the compressed fuel-air mixture will leak away during each compression stroke, resulting in an effectively larger compression volume. Since this leakage is time-dependent, the actual compression ratio increases with the rotational speed of the crank. Based on a previous measurement of the characteristics of the modified engine running on Diesel fuel at 240 rpm, the compression ratio is roughly derived to be about 1:9, assuming a simple adiabatic compression stroke. This is small in comparison with the standard values near 1:16 and most likely caused by the modifications providing the optical accessibility of the cylinder. Due to the movement of the piston the windows in the cylinder wall are optically blocked for crank angles between 50° b.TDC (before Top Dead Centre) and 50° a.TDC, thereby limiting the 2D-LIF measurements in the expansion stroke to crank angles greater than 50° a.TDC after combustion. The maximum delivered power of the engine was measured using the adjustable brake to increase the load until the engine ceased running. In the case of $n$-heptane this turned out to be almost 1.8 kW, whereas in the case of Diesel fuel this limit dropped to about 0.9 kW. In both cases the piston was overheated and got slightly stuck near BDC (Bottom Dead Center). The highest measured power (1.8 kW) is used as the reference value, to be called 100% load. At present the engine is being modified in order to increase the maximum power to the originally rated value of approximately 6 kW.

The tunable ArF-excimer laser (Lambda Physik EMG 150 MSCT) depicted in Fig. 1 actually consists of two laser

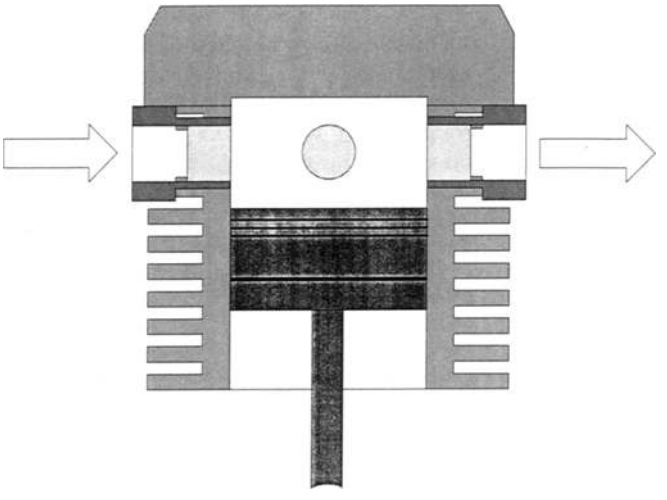

**Fig. 2.** The optical accessibility of the cylinder. The laser beam travels from left to right and the 2D-LIF signal is detected in the perpendicular direction. The cross section of the swirl chamber in the cylinder head is not drawn

tubes, one serving as a tunable oscillator and the other as an amplifier for the oscillator radiation. This amplifier may be used in either Single-Pass (SP) mode (typically 40 mJ/pulse) or Multiple-Pass (MP) mode, the latter mode resulting in more power (typically 100 mJ/pulse) at the expense of the spectral purity of the laser output [4]. To increase the S/N ratio of the imaging in this work the amplifier is set to operate in SP mode delivering narrow-band tunable laser pulses with a spectral intensity around 5 MW/cm$^2$ if tuned near the centre of the 300 cm$^{-1}$ wide tuning range. The bandwidth of the laser is about 0.6 cm$^{-1}$ as derived from measurements on NO in an oxy-acetylene flame used for on-line calibration of the laser frequency.

By means of two 45° mirrors the laser beam is vertically adjusted to the position of the windows in the cylinder wall. About 8% of the laser energy is directed into the calibration section of the setup, using a $MgF_2$ beamsplitter. Without the optional insertion of the two cylindrical lenses (depicted in Fig. 1) the pulse energy measured at the entrance window of the engine is approximately 30 mJ. During operation the laser beam is attenuated by a factor of 2 due to a thin layer of soot on the entrance window and the resulting intensity inside the cylinder is about 1.9 MW/cm$^2$ in a 20 mm high and 3 mm wide rectangular cross section. Inserting the two lenses and keeping the cross section unaltered yields about 20 mJ/pulse at the entrance window and an operational in-cylinder intensity of about 1.3 MW/cm$^2$, which turns out to be too low to produce the same signal strength compared to the case in which the laser beam is not modified. Focusing the laser beam into thinner sheets leads to slightly stronger signals, which is an indication that the invoked transition is not saturated at these pulse energies.

Within the tuning range of the laser NO can be efficiently excited through many rotational channels of the electronic-vibronic transition: $D^2\Sigma^+(v' = 0) \leftarrow X^2\Pi(v'' = 1)$. Due to collisional quenching, however, the slightly lower level $C^2\Pi(v' = 0)$ will be populated as well and the resulting fluorescence displays two clearly distinguishable sequences: $D^2\Sigma^+(v' = 0) \rightarrow X^2\Pi(v'' = 2,3,4,5,6)$ and $C^2\Pi(v' = 0) \rightarrow X^2\Pi(v'' = 1,2,3,4,5,6)$, the strongest one originating from the primary excited level. The fluorescence resulting from the $D^2\Sigma^+(v' = 0) \rightarrow X^2\Pi(v'' = 3)$ transition of NO at 208 nm is selected for performing the 2D-LIF measurements as well as for the on-line calibration. The 2D-LIF signal is slightly magnified by a spherical lens ($f = 10$ cm) and subsequently transmitted through a band-pass interference filter consisting of four dielectric coated mirrors. The filter is adjusted to a maximum transmission of 80% at 208 nm with a bandwidth of 10 nm. This filtered 2D-LIF signal (imaging an in-cylinder area with a diameter of about 2 cm) is then fed to a 50 ns gated image intensifier and either directly processed or recorded on videotape for later processing. The calibration is achieved by measuring the time averaged intensity of the LIF signal (gate 100 ns) resulting from the same transition of NO in an oxy-acetylene welding torch by means of a 25 cm focal-length monochromator (Jobin Yvon M25, 610 g/mm) set to 208 nm and a photomultiplier (EMI 9635 QB), using the calibration data produced by Versluis et al. [4].

The imaging software is written for use with a specific image processing board (Matrox PIP-1024 A/D converter) installed in a 80386 AT personal computer. This board has an 8 bits dynamical range (256 grey values) and produces pictures of $512 \times 512$ pixels on the screen of a separate RGB monitor (Sony Trinitron). The software provides the possibility of false colour representations using different selectable pixelvalue-to-colour conversions. In addition to all basic picture modifying functions provided by the software, this system is also capable of taking its input from a VHS video recorder. This turned out to be a very convenient option at the expense of a hardly noticeable decrease of the S/N ratio and consequently all 2D-LIF measurements in this work are processed afterwards from video tape. Another relevant feature of the software is the option to add all pixel values within a selectable rectangle of continuously grabbed images, thereby calculating the total intensity of each grabbed area. Each calculated value is plotted on the computer screen before the next picture is grabbed, creating an excitation spectrum if the laser is scanned simultaneously over its tuning range. All excitation spectra presented in this work are obtained using this procedure and the recording time for each of the two excitation spectra obtained from the running engine was about 15 min. In a similar way the software is capable of adding any number of grabbed images and dividing the obtained array of total pixel values by the number of grabbed images to produce an averaged picture. A sophisticated re-scaling by fractional factors of this array to the full dynamical range is another option of the software which was used to obtain the averaged NO distributions under varying combustion conditions at specific crank angles. In this case the laser is tuned to a specific resonance and all other variables are kept constant during at least 2 min for each presented averaged NO distribution.

## 2 Results and Discussion

All 2D-LIF measurements were performed for oxygen enriched combustion. The calibration signal was recorded on a strip-chart recorder while the 2D-LIF signals were simultaneously recorded on video tape using the maximum gain of the image intensifier. The intake air was buffered to achieve a more efficient and continuous oxygen supply for all rotational speeds and as a result of this buffering precise oxygen volume fractions could not be determined. Volume fractions ranging from 30% to 40% seem reasonable estimates for most of the presented measurements.

For each fuel an excitation spectrum was recorded by scanning the laser frequency, whereafter several averaged NO distributions (at specific crank angles and specific loads) were measured at one of the strongest resonant rotational transitions. Data of Lee et al. [5] concerning interfering absorptions of the laser beam by molecular oxygen (around 193 nm), show that rather strong and temperature dependent absorptions may occur within the whole scanning range of the laser. These authors found, however, that one specific rovibronic transition of NO is undisturbed by absorption even at very high temperatures of the oxygen in the combustion. Although these strong absorptions were not observed in the engine this transition ($R_1(26.5)/Q_1(32.5)$ at 193.377 nm) [4] was selected to image the averaged NO distributions.

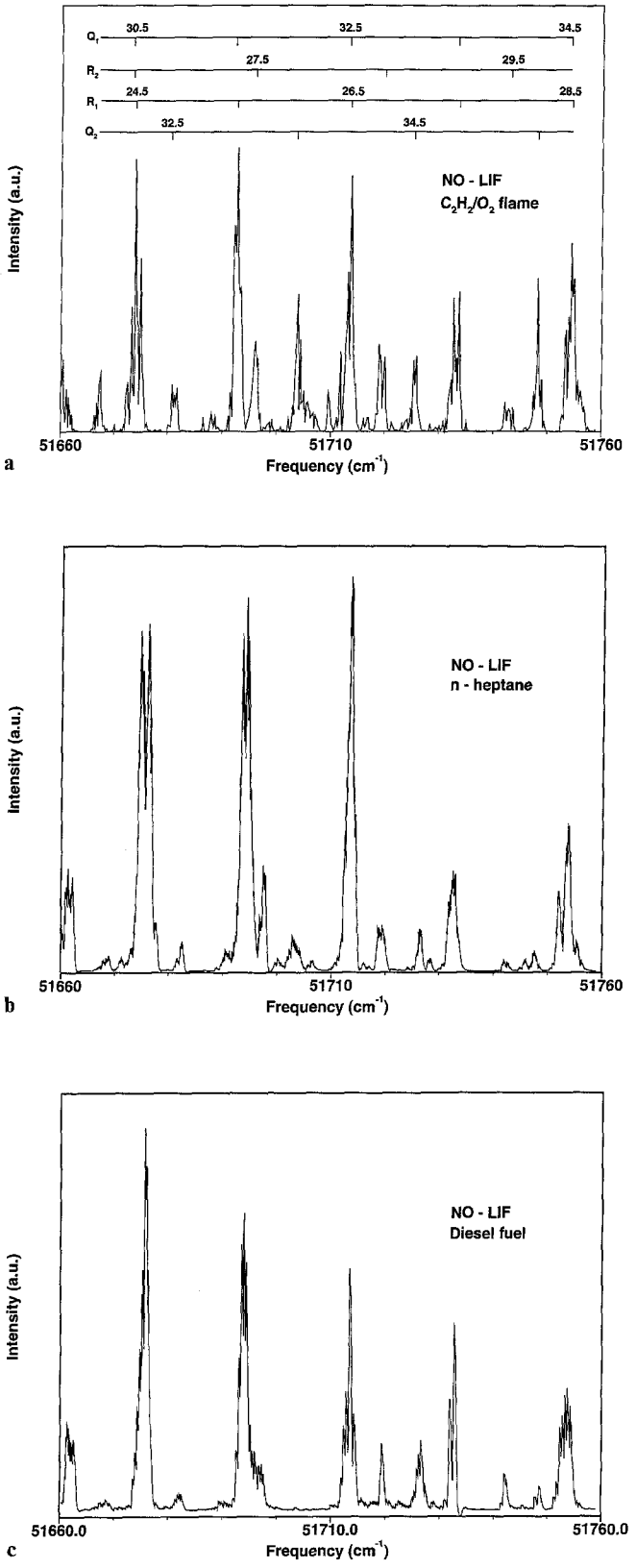


**Fig. 3.** **a** The $D^2\Sigma^+(v'=0) \leftarrow X^2\Pi(v''=1)$ excitation spectrum of NO, as obtained from an oxy-acetylene welding torch using the 2D-LIF technique. The identification of the rotational transitions is indicated by the *horizontal bars* on top of the spectrum; **b** excitation spectrum of NO, as obtained from the $n$-heptane driven Diesel engine (1000 rpm, 25% load, at BDC after combustion); **c** excitation spectrum of NO in the case the engine is driven by Diesel fuel (720 rpm, 25% load, at BDC after combustion)

The measured 2D-LIF excitation spectra are compared to a significant part of the complete excitation spectrum as it is measured by Versluis et al. [4]. For a fair comparison, that particular part of the spectrum was remeasured in a welding torch, applying the same 2D-LIF technique as used for all other measurements in this work. This spectrum is given in Fig. 3a where the relevant rotational transitions are indicated by bars on top of the spectrum. The strongest progression in all excitation spectra actually consists of two nearly coinciding sequences of transitions starting from different rotational levels in the ground state [4]. The $R_1$ progression departs from lower rotational levels, whereas the $Q_1$ transitions occur from higher rotational levels. Because of collisional quenching one must be careful in drawing conclusions from the intensity differences of the lines of this progression. The significantly lower intensity of the $R_1(27.5)/Q_1(33.5)$ transition, however, might be due to the stronger absorption by molecular oxygen at that wavelength [5].

The excitation spectra from the engine are presented in Figs. 3b, c, using $n$-heptane and Diesel fuel, respectively. Both spectra were recorded at BDC after combustion and as the exhaust valve is opened at that time, the pressure is expected to be slightly higher than atmospheric pressure. The engine delivered the same power (25% load) during these recordings resulting in different rotational speeds: 1000 rpm combusting $n$-heptane and 720 rpm running on Diesel fuel. The $S/N$ ratio of both spectra is sufficiently high to characterize the recorded images as being produced by hot NO ($v''=1$). A comparison with the flame spectrum shows that the $Q_2$ progression originating from high rotational states is weaker, which must be the result of a lower temperature in the engine. Another difference between the flame and engine spectra is given by the linewidths. In particular for n-heptane broad lines are observed with a width of about 1.5 $cm^{-1}$. A possible explanation might be given by different contributions of the $R_1$ and $Q_1$ transitions to the lineshape. At the high flame temperature the $Q_1$ lines will be stronger than the $R_1$ transitions whereas at the lower engine temperatures both the $R_1$ and $Q_1$ transitions may give comparable contributions to the total line intensity. Since the frequencies of the $R_1$ and $Q_1$ transitions are slightly different ($\sim$0.5 $cm^{-1}$) a line broadening may result. In contrast to the spectrum from the welding torch (Fig. 3a) a small background signal is observed in the spectra from the engine. This is assumed to originate from fuel fragments radiating, either spontaneously or laser induced, within the bandwidth of the 2D-LIF filter (203–213 nm).

Some of the measured two-dimensional NO distributions at specific crank angles as a function of the engine load are depicted in Fig. 4. The laser beam travels from left to right in all pictures and the same vertical plane in the cylinder is imaged by these measurements (blue represents a lower local intensity and red indicates the highest local intensity). All averaged distributions are obtained by grabbing more than 100 frames and re-scaling the result to the full dynamical range of the image processing system. The display of these results is organized in the following way: the top row (a–c) was measured at 60° b.BDC, 45° b.BDC and at BDC, respectively, using $n$-heptane and no load at 1300 rpm. The second row (d–h) resulted from measurements at the same

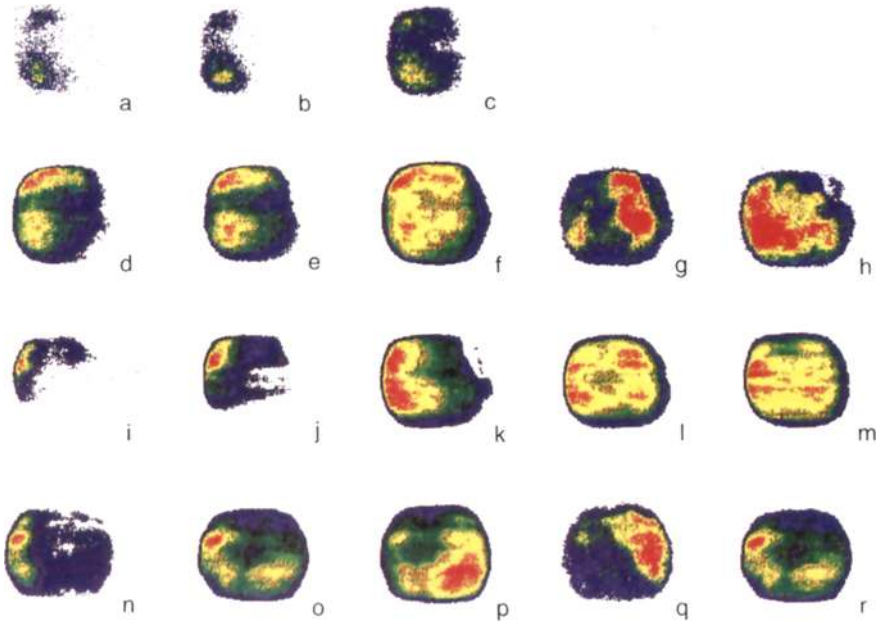


**Fig. 4a–r.** Averaged NO distributions and typical single snapshots measured as a function of crank angle, engine load and fuel; **a–c** averaged NO distributions in $n$-heptane combustion at 60° b.BDC, 45° b.BDC and at BDC after combustion, respectively, without load at 1300 rpm; **d–f** similar to **a–c** but with 25% load at 1200 rpm; **g** and **h** single snapshots of the NO distribution at BDC in $n$-heptane combustion with 50% load at 1100 rpm; **i–m** averaged NO distributions in $n$-heptane combustion at 60° b.BDC, 45° b.BDC, BDC, 30° a.BDC and 60° a.BDC, respectively, with 52% load at 1100 rpm; **n–p** averaged NO distributions in Diesel fuel combustion at 60° b.BDC, 45° b.BDC and BDC, respectively, with 25% load at 700 rpm; **q** and **r** single snapshots of the NO distribution at BDC in Diesel fuel combustion with 25% load at 700 rpm

crank angles, using $n$-heptane and 25% load at 1200 rpm. The last two pictures of this row (g and h) are arbitrary single snapshots at BDC after combustion, using $n$-heptane and 50% load at 1100 rpm. The third row (i–m) shows the results at the same crank angles as in the previous two rows, using $n$-heptane and 52% load at 1100 rpm. The last two pictures of this row (l and m) are measured in the exhaust stroke at 30° a.BDC and 60° a.BDC, respectively, under the same circumstances as all others in this row. The bottom row (n–r) displays the results at the same crank angles as all previous rows, but now using Diesel fuel and 25% load at 700 rpm. The last two pictures of this row (q and r) are (again) arbitrary single snapshots at BDC, using Diesel fuel and 25% load at 700 rpm.

The highest occurring pixel value in all snapshots is typically about 64, indicating a reasonable signal strength (25% of the full dynamical range) mainly limited by the laser intensity, since the transition does not appear to be saturated. To study the intensity dependence of the 2D-LIF signal on the crank angle the total averaged intensities of the unscaled signal of the two bottom rows are compared to the averaged intensity at BDC. This yields for the third row: (i) 4%, (j) 20%, (k) 100%, (l) 240%, (m) 200% and for the fourth row: (n) 6%, (o) 13% and (p) 100%. In both cases the averaged total intensity increases fast as the pressure decreases which is a result of the higher quantum yield of the transition at lower pressures due to reduced collisional quenching. A similar pattern is displayed by the first two rows (a–c, d–f). The total averaged intensity as measured at BDC using Diesel fuel and 25% load at 700 rpm turns out to be about twice as strong as the total averaged intensity at BDC using $n$-heptane and 52% load at 1100 rpm. Due to the re-scaling these total intensity differences are hardly reflected in the presented pictures of the averaged distributions.

In principle the measured pictures reflect the distribution of hot NO ($v'' = 1$) in the plane of the laser sheet. The exhaust valve in the cylinder head happens to be mounted at the side of the laser entrance window (left), while the inlet valve is mounted on the right. Moreover, the right side of the cylinder is more efficiently cooled because the cooling-fan is positioned there. This may explain the mostly stronger intensity observed at the left hand side of the pictures. However, the observed intensity distribution may be influenced by absorption of the laser beam along its path in the combustion chamber. If this were the case a stronger signal intensity from the left side of the viewed area should always be observed. Although most times the signal from the left hand side is the strongest indeed, this is not always the case as can be seen in the snapshots (g) and (q) as well as in the averaged distribution (p). So absorption along the length of the viewing area does not seem to play an important role and the observed inhomogeneous distributions are most probably due to asymmetries in the NO distribution. In order to prove this argument the direction of the laser beam will be reversed in future experiments. In some pictures of averaged distributions areas of lower total intensity (like d, e and f) are probably due to a non-homogeneous distribution of the pulse energy over the cross section of the laser sheet once the sheet has entered the cylinder. The different combustive behaviour of both fuels is reflected in the clearly different pictures of averaged NO distributions (k) and (p). In the case of Diesel combustion (p) the NO distribution is more intense at the right hand side. Experiments are in progress to find the origin of this phenomenon.

## 3 Summary

The imaging of NO distributions inside a running Diesel engine by 2D-LIF measurements extended to longer periods of time offers the opportunity to investigate different combustion processes as they result from selected fuels and operating conditions. In this work it is shown for the first time that NO produced in the combustion of Diesel fuel can be observed. This is of importance for future laser diagnostics in Diesel engines as well as in other Diesel combustion processes. The use of substitute fuels like $n$-heptane does not result in improved NO images, as was expected in view of increased absorption of laser radiation and emissions by many different components in the Diesel fuel. The different combustive behaviour of $n$-heptane and Diesel fuel in the same engine was observed in the total averaged intensities of the 2D-LIF signals as well as in the averaged spatial NO distributions at BDC.

The total observed 2D-LIF signal intensity appears to be limited mainly by the low laser power which was used to enhance the spectral purity of the measurements. Future experiments will be performed using increased laser power since the loss of spectral purity is balanced by much stronger 2D-LIF signals once the molecular source of the imaged radiation is identified. In addition, the load will be increased by modifying the engine, which will result in more realistic (i.e. larger) NO concentrations. This will allow the study of the NO formation in an earlier stage of the combustion process. In future experiments the tailpipe $NO_x$ concentration will be measured as well in order to estimate the in-cylinder NO concentration resulting from selected steady operating conditions.

*Acknowledgements.* The support of NOVEM B.V., Utrecht, The Netherlands is gratefully acknowledged. We further thank Mr. E. van Leeuwen and Mr. F. van Rijn for their expert technical assistance and Mr. K. Schreel for his help in producing the figures in this manuscript.

## References

1. P. Andresen, G. Meijer, H. Schlüter, H. Voges, A. Koch, W. Hentschel, W. Oppermann, E. Rothe: Appl. Opt. **29**, 2392 (1990)
2. A. Arnold, F. Dinkelacker, T. Heitzmann, P. Monkhouse, M. Schäfer, V. Sick, J. Wolfrum, W. Hentschell, K.P. Schindler: 24th Int'l Symp. on Combustion, Sydney (1992)
3. B. Alatas, J.A. Pinson, T.A. Litzinger, D.A. Santavicca: SAE Paper 930973 (1993)
4. M. Versluis, M. Ebben, M. Drabbels, J.J. ter Meulen: Appl. Opt. **30**, 5229 (1991)
5. M.P. Lee, R.K. Hanson: J. Quant. Spectrosc. Radiat. Transfer **36**, 425 (1986)